Materials Transactions, JIM, Vol. 37, No. 4 (1996), pp. 663 to 669
Paper from JIM '95 Fall Annual Meeting in Hawaii

Phase Stability under High-Pressure in two Precipitation Strengthened Alloys

Marcel H.F. Sluiter*, Y. Watanabe, and Y. Kawazoe
Institute for Materials Research, Tohoku University, 2-1-1 Katahira, Aoba-ku, 980 Sendai, Japan

The effect of hydrostatic pressure on the stability of precipitates in the Al-Li and Cu-Be alloy systems has been examined using a first-principles method. The solid-phase portion of the Cu-Be and Al-Li phase diagrams has been computed from first-principles. In the case of Cu-Be no adequate description of the thermodynamics could be obtained, and consequently no realistic phase diagram could not be computed. However, an analysis of a Calphad type calculation indicates why the current method fails. For Al-Li a good cluster expansion could be obtained and the computed zero pressure phase diagram exhibited excellent agreement with the experimental data. A high pressure phase diagram was computed as well. It is predicted that phase equilibria in the Al-Li system are little affected by compression. Compression does not affect the Al - Al_3Li metastable phase equilibria but the calculated equilibrium isothermal solubility of Li in Al is decreased, in agreement with recent measurements.

Keywords: pressure dependence of phase equilibria, Al-Li alloys, Cu-Be alloys, theory of alloy phase stability, enthalpies of formation, cluster variation method

I. INTRODUCTION

In alloys where the precipitating phase is metastable, or where the precipitating phase has a bulk modulus or density which differs much from the matrix, hydrostatic stress may greatly affect the relative stability and formation of the precipitates. In a commercial Cu-Be alloy it has been reported that application of a pressure of about 7.5 GPa reduced the Be solubility in Cu by as much as half and greatly influenced the rates and appearance of precipitation[1]. In Al-Li alloys too, a pronounced pressure dependence of the Li solubility in Al has been reported recently[2]. For most alloy systems little information is available on the pressure dependence of phase equilibria. Therefore the ability to predict the effect of hydrostatic pressure on the phase diagram is of practical use. In this paper it will first be attempted to compute the zero-pressure phase diagram from first-principles, i.e. without the use of any experimental data. When such a first-principles result agrees with the assessed experimental phase diagram, a first-principles high-pressure phase diagram is computed as well, and the effect of pressure on the phase equilibria is determined.

The stable and metastable phase equilibria in the Al-Li[3–10], and Be-Cu[11,12] systems have been well studied. Nevertheless, it is of interest to attempt to compute phase equilibria in these well-known alloy systems from first principles because once a good theoretical description is obtained the effect of various "perturbations", such as hydrostatic stress, for which little experimental data is available, can be easily incorporated in the theoretical description allowing predictions, rather than verifications.

Pressure dependent calculations in the Al-rich side of the Al-Li system and the Cu-rich side of the Cu-Be system are simplified by the fact that the relevant phases all have cubic symmetry, which means that there is a simple relationship between lattice parameter and hydrostatic pressure. The effect of pressure is of interest both in its own right, and also because it may indicate whether other states of stress affect the phase equilibria. In cases where phase equilibria show a strong response to hydrostatic stress, it is plausible that under actual loading the stability of phases, e.g. phases precipitated during age hardening, can be affected. These issues are especially relevant in the case of Al-Li and Cu-Be alloys where the mechanical properties are enhanced through precipitation. It has been reported that hydrostatic pressure can greatly affect the nature and distribution of precipitates[1]. Moreover, recently, a portion of the Al-Li high-pressure phase diagram has been determined experimentally[2], so that some of the computational results can be verified.

The current method can be summarized as follows: The total energies of selected ordered supercells are computed for various values of the lattice parameter (i.e. volume per atom) with the LMTO-ASA method[13]. Minimizing the energy with respect to the lattice parameter yields for each ordered structure the equilibrium values of the lattice parameter and the total energy. The bulk modulus is obtained from the curvature of the total energy with respect to the volume.

Total energies are used to extract chemical interaction energies[9] between the Al and Li species in various crystalline environments as a function of the volume per atom. This method of extracting interactions from total energies has been applied previously to several systems such as: Al-Ti[14], Cd-Mg[15], Pd-V[16], Ni-Pt[17–20], Ni-Al

and Cu-Pd[21]. The interactions are the coefficients in an Ising-type Hamiltonian, which is solved in an approximate manner, in this case with the Cluster Variation Method (CVM)[22–24]. "Solving this Ising-like Hamiltonian" means that configurational free energies are computed for each state of order, composition, and temperature. Finally, by combining the configurational free energies of various phases the composition-temperature, or the composition-pressure phase diagram is constructed. The necessity for an underlying lattice limits the current description to crystalline phases.

In accounting for the hydrostatic pressure it is assumed that the global volume relaxation only is of importance for each superstructure. Of course for non-cubic structures, such as the tetragonal $L1_0$ phase, and for structures with cell internal degrees of freedom, such as the complex Al_2Li_3 phase, this is an approximation. However, the stable and metastable phases of interest in the alloy systems have cubic symmetry (fcc, $L1_2$, B32, bcc, B2), so that this approximation is not likely to be of significance. Moreover, in the Al-rich alloys which are of particular interest, Al and Li have the same partial molar volumes which indicates that relaxations are very small. For example, when the c/a ratio of the hypothetical tetragonal Al_3Li DO_{22} phase is computed, a value of 1.974 is found which differs insignificantly from the ideal ratio of 2. The c/a relaxation in this phase decreases the total energy by a paltry 16 J/mol. Hence, the approximation of ignoring deviations from the exact fcc (bcc) lattice positions (volume relaxation is treated only) is well-justified in Al-rich alloys.

In Cu-rich Cu-Be alloys a similar argument can be made. The lattice parameter in the Cu-rich fcc phase does not depend strongly on the Be concentration[12], and the computed c/a ratio for a hypothetical DO_{22} Cu_3Be phase is 1.99 and the corresponding change in the total energy is just 59 J/mol.

In the current method configurational and static displacement effects are considered only. The effect of phonons is neglected. This neglect should not generally be valid and below we will discuss how vibrational effects might affect our findings.

II. METHOD

Total energies of a large number of fcc and bcc superstructures were computed with the LMTO-ASA method[13]. Equal sphere radii were selected for all atoms, the "combined corrections" to the ASA were included, the maximum angular momentum considered was 2 (spd basis), and the von Barth-Hedin parametrization of the exchange correlation potential was used. Care was taken to compute all superstructures with the same k-point grid, which included 1000 points in the 1st Brillouin zone for the fcc- and bcc-based crystal structures. Formation energies ΔE_{form} were extracted from the total energies E_{tot} by subtracting the concentration-weighted average of the total energies of the pure elements in the fcc state, according to

$$\Delta E^{\alpha}_{form}(V) = E^{\alpha}_{tot}(V) - c^{\alpha}_{B} E^{B-fcc}_{tot}(V_o) - (1 - c^{\alpha}_{B}) E^{A-fcc}_{tot}(V_o) \quad (1)$$

where the superscript α refers to a particular superstructure, c^{α}_{B} is the concentration of the B species in the α phase, V is the volume per atom, and V_o refers to the equilibrium value of V. Here, we have selected the fcc crystal structure as reference state. The actual Li and Be ground states are the close packed $9R$[25] and the hcp structures. However, this is of little consequence because we are interested in phase equilibria at Al- and Cu-rich compositions. At constant, non-zero pressure, enthalpies H, rather than energies need to be considered. Enthalpies of formation ΔH_{form} can be computed with

$$\Delta H^{\alpha}_{form}(P) = H^{\alpha}(P) - c^{\alpha}_{Al} H^{Al-fcc}(P) - (1 - c^{\alpha}_{Al}) H^{Li-fcc}(P) \quad (2)$$

where P is the hydrostatic pressure, and the enthalpy itself is given by

$$H^{\alpha}(P) = E^{\alpha}_{tot}(V(P)) + PV(P). \quad (3)$$

The volume V is found by solving $P = -\frac{\partial E_{tot}}{\partial V}$. At finite temperature one solves $P = -\frac{\partial F}{\partial V}$ to find V, where F is the Helmholtz free energy of formation ($F = E_{form} - TS$).

The total energies are used to obtain effective cluster interactions (ECI) by means of a Connolly-Williams procedure[26]. The ECI J_i for a cluster i are calculated with

$$\sum_{\alpha} w^{\alpha} [\Delta E^{\alpha}_{form}(V) - \sum_{i=1}^{n} J_i(V) \xi_i{}^{\alpha}]^2 = minimal \quad (4)$$

where ξ is the cluster correlation function as defined in equation 10 in Ref.[9], and w represents the weights assigned to each structure[27].

Finally, the energy of any superstructure can be computed with

$$\Delta E^{\alpha}_{form}(V) = \sum_{i} \xi_i{}^{\alpha} J_i(V). \quad (5)$$

The convergence of the cluster expansion of the formation energy has been checked by computing the predictive error[27]. The predictive error was less than 2.0 (2.6) kJ/mol corresponding to a relative error in the formation energy of about 20 % (11 %) on the fcc (bcc) lattice for the Al-Li system, and for Cu-Be the predictive error was 1.2 (3.5) kJ/mol or 10 % (16%) on the fcc (bcc) lattice.

For the fcc lattice, the following set of 14 structures was used to extract the ECI: fcc, $L1_0$, $L1_2$, K40, DO_{22},

TABLE I. Structural energy difference $E^{fcc-bcc}$ in kJ/mol for the pure elements

element	$E^{fcc-bcc}$		
	this work	FLAPW	Calphad
Al	4.03	6.04[9]	10.1[3]
Be	-1.87	-	2.66[38,11]
Cu	0.68	3.0[39]	3.0[31] 3.56[38] 6.28[11]
Li	0.37	0.66[9] 0.26[34]	-1.2[3]

C2/m AB_5 and A_2B_4[28], and $C11_b$ ($MoPt_2$ prototype). K40 refers to structure nr 40 in the fcc ground state analysis by Kanamori and Kakehashi[29]. On the bcc lattice a set of 19 structures was used to compute the ECI in the Al-Li system: bcc, B2, B32, DO_3, $C11_b$ ($MoPt_2$ prototype), B11, F9, F10, F13, F17, unrelaxed Al_4Li_9 and Al_9Li_4, where the structures with prefix "F" refer to ground states discovered by Finel[30]. The bcc ECI in the Cu-Be alloy were computed with a set of 14 structures: bcc, B2, B32, DO_3, $C11_b$ ($MoPt_2$ prototype), B11, F5, F9, F10.

The energies of formation for structures in both sets were reproduced to within 0.5 kJ/mol by the fcc and bcc cluster expansions, eq. 5. The ECI were used to compute the formation enthalpies of all known ground state structures[29,30] and no additional ground states could be found.

The phase equilibria at non-zero temperature were determined with the Gibbs free energy

$$G^\alpha = H^\alpha - TS^\alpha \tag{6}$$

where T and S are the temperature and entropy, respectively.

The tetrahedron approximation of the CVM was found to be insufficient to accurately represent the states of order and the associated energies of formation. Instead, the tetrahedron-octahedron maximal clusters[28] were used for the fcc and its superstructures, and the centered tetrahedron-octahedron-pentuplet (TOP) maximal clusters were used for the bcc and its superstructures[27].

III. RESULTS

A. Phase Stability at zero Temperature

The structural energy differences between fcc and bcc for the pure elements as computed with the LMTO-ASA are compared with those obtained with other methods in Table III A.

Clearly, agreement between the various methods is poor. This is a well-known occurrence[31]. In the case Li there is not even agreement on the sign. The positive sign as computed in the LMTO-ASA and FLAPW[9] is almost certainly correct because the actual ground state is the close packed 9R structure which should be almost degenerate with the fcc structure. For Cu it must be assumed that the FLAPW calculations are more accurate than the LMTO-ASA because in the latter additional shape approximations are made in the potential and charge density.

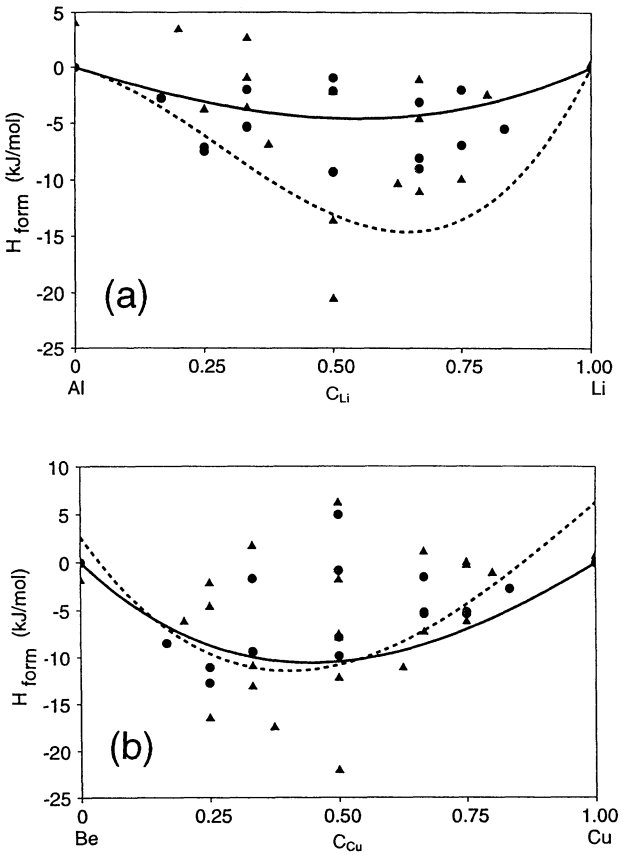

FIG. 1. Formation enthalpies of fcc (circles) and bcc (triangles) superstructures as computed with the LMTO-ASA for the Al-Li system (a) and the Cu-Be system (b). Two independent assessed formation enthalpies of the fcc SS are shown also in (a):from Ref. 5 (solid line), from Ref. 3 (dashed line). For Cu-Be the assessed formation enthalpies[11] for the fcc (solid line) and bcc (dashed line) SS have been shown.

The formation enthalpy of a solid solution (SS) at low temperature tends to closely follow the convex hull of the ground states of the pertinent underlying lattice. Thus, it is meaningful to compare the energies of formation of the fcc and bcc superstructures with the enthalpy of formation as obtained in the Calphad approach. In Figure 1 the enthalpies of formation at zero temperature are shown.

For Cu-Be, the enthalpies of the fcc ground states are all close to the assessed curve[11]. The formation enthalpies of bcc ground states, however, tend to be much more negative than the assessment, although the assessed curve has an asymmetry which displaces the minimum towards the Be-rich side, just like the ordered structures. Experimental data[32] of the Gibbs free energy at 1073

K of the fcc, bcc and B2 phases indicates that the enthalpies of formation on the fcc and bcc lattices should be about the same. The formation Gibbs free energy of the B2 CuBe phase at 1073 K is about 15 kJ/mol[32]. Considering that at a temperature so close to the experimental order-disorder temperature significant configurational entropy is present, the zero temperature enthalpy of formation should be less than 15 kJ/mol. Therefore, it appears likely that the LMTO-ASA value of the formation enthalpy (22.1 kJ/mol) is too large. The large enthalpies of formation computed for bcc-based structures will strongly impact the computed phase diagram, as will be detailed below.

Two assessments are available for the Al-Li system. Since there is no bcc SS, only the assessed[3,5] fcc enthalpy of formation is shown. Clearly, the two assessments differ significantly from each other, but the convex hull of fcc based ground states lies quite neatly between the two assessments. It appears that for the Al-rich alloys of interest here, the curve from Ref.[3] is in better agreement with the LMTO-ASA results.

B. Phase Diagrams at zero Pressure

The solid phase portion of the Al-Li phase diagram at zero hydrostatic stress is shown in figure 2a. To facilitate comparison with experiment, the "interloper" Al_2Li_3 and Al_4Li_9 phases were included.

At zero pressure, the only stable fcc- and bcc-based phases are computed to be Al-rich fcc, AlLi B32, and at the Li-rich side both fcc and bcc. In addition, the metastable Al_3Li $L1_2$ phase, often referred to as the δ' phase, and its two phase region with the Al-rich fcc SS have been shown. The Li solubility limit in the Al-rich SS and the width of the B32 single phase region are underestimated. Except for those quantitative differences, the agreement with the solid-phase part of the experimental phase diagram is striking. The correct phases are indicated and their composition and temperature ranges are qualitatively correct. The computed Al_3Li $L1_2$ order-disorder temperature is just above the highest temperature at which $L1_2$ precipitates are observed, and the fcc - $L1_2$ two phase region exhibits a good qualitative agreement with that determined in actual alloys[5]. The low temperature metastable miscibility gap (MG) for Al-rich fcc based alloys, which has been postulated in previous work[6,7], has been found. However, it must be remarked that this feature is associated with a very small energy difference, which is several orders smaller than the predictive error of the cluster expansion. Therefore, the MG is rather speculative and it might easily disappear with a more accurate expansion. It should be noted though that without such a low temperature MG, the fcc - $L1_2$ two phase region tends to be much narrower[9] than is experimentally observed.

About the quantitative shortcomings of the computed

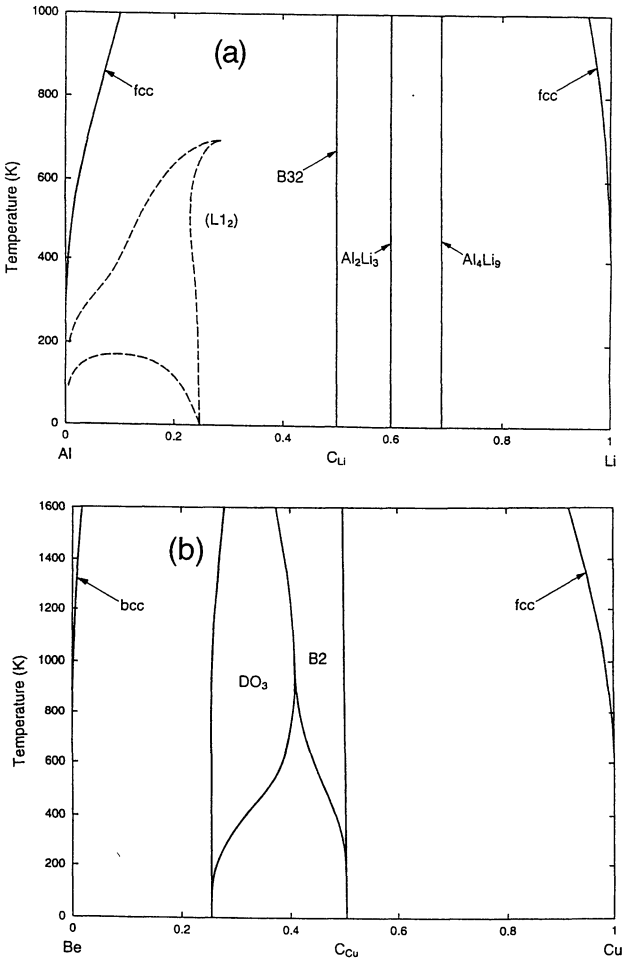

FIG. 2. The solid portion of the Al-Li (a), and Cu-Be (b) phase diagram at zero pressure; binodals (solid lines), metastable phase boundaries (dashed lines).

phase diagram, we note the following: The too low value for the Li solubility limit in the fcc SS might be due to the neglect of the vibrational degrees of freedom. We expect the free energy of the SS to be lowered more than that of the B32 phase because the SS has a lower melting point, and because the stiffness of the B32 structure is greater than the average of its constituents. Recently Garbulski and Ceder[33] have shown that, in the harmonic approximation, the ECI at high temperature can be modified considerably when the spring constants between unlike atomic species differ from the geometric mean. The high relative stiffness of the B32 phase destabilizes it with respect to less stiff competing phases because those phases lower their free energies more by vibrations than the B32. Neglect of vibrational effects is also responsible for the absence of an fcc to bcc transformation at finite temperature in pure Li.

In the case of Cu-Be, the first-principles predicted phase diagram, see figure 2b, differs more significantly from the assessed experimental data[11,12] On the Be-rich side the C15 type Laves phase of stoichiometry $CuBe_2$ has been excluded, but at the Cu-rich side too, agreement is poor. In particular, the current calculation fails to produce the bcc SS between the fcc Cu-rich SS and the CuBe B2 ordered phase, and the computed order-disorder temperature of the B2 CuBe phase is about 2.6 times higher than observed. Another, less significant difference is that the prediction much underestimates the Be solubility in fcc Cu. Both the much too high predicted B2 order-disorder temperature and the underestimated solubility of Be in fcc Cu are a direct consequence of the large B2 formation enthalpy as computed with the LMTO-ASA. In a future study, the origin for the apparent too large formation enthalpies for bcc based structures will be examined. The effect of pressure on the Cu-Be system has not been considered because no satisfactory description is obtained at zero pressure.

It should be mentioned that apparently the Cu-Be system is not easily modeled. Although the Calphad approach yields a phase diagram that displays fair agreement with experiment, is does so with rather unphysical features. In particular the bcc Cu-rich SS is made to appear in the phase diagram by assuming a most unusual composition dependence of the entropy. In figure 3 the entropy of mixing is shown for fcc and bcc SSs as given by the Calphad parametrization[11]. Notice that the fcc entropy is about twice that of a random SS, and that the bcc entropy displays a decrease as a function of composition when Cu is added to Be, and the pronounced maximum towards to the Cu-rich side is responsible for stabilizing the high temperature Cu-rich bcc SS. These features of the entropy of mixing appear rather unlikely.

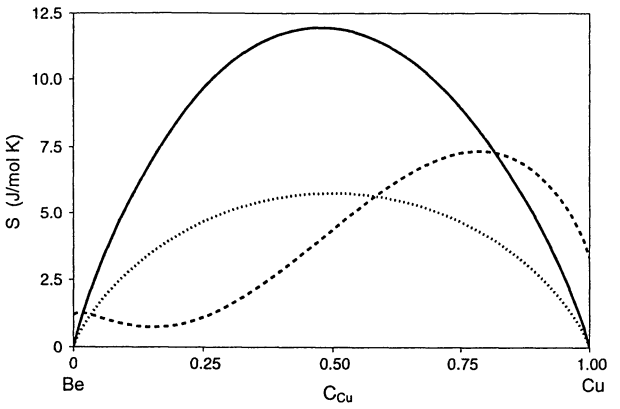

FIG. 3. Entropy of mixing according to the assessment by Kaufman and Tanner [11] as a function of composition. Fcc (bcc) Cu-Be SS: solid (dashed) line, ideal configurational entropy: dotted line.

C. Al-Li Phase Equilibria at 5.4 GPa

As was reported previously[9], the technologically important Al-fcc and Al_3Li $L1_2$ phases are computed to have nearly identical lattice parameters, in agreement with the experimental observation that the $L1_2$ phase forms perfectly coherent spherical precipitates. At a hydrostatic pressure of 5.4 GPa the already small lattice mismatch decreases very slightly. Hence, it is expected that the morphology of the Al_3Li precipitates in Al-rich fcc matrix is unaffected by pressure. Of course, comparing the lattice parameter of stoichiometric $L1_2$ with that of pure fcc Al is not quite correct because in the actual alloy the compositions of the $L1_2$ and fcc matrix are not stoichiometric or pure.

At 5.4 GPa hydrostatic pressure, the ground states on the Li-rich side change: On the fcc lattice the $L1_0$ AlLi structure is replaced by the K40 ground state, which is almost degenerate with the $L1_0$ state of order, and at composition $AlLi_3$ a marginally stable DO_{22} ground state emerges. On the bcc lattice, the B32 strucΦure remains by far the most stable ordered state, but compression stabilizes the $AlLi_3$ DO_3 phase sufficiently to break the convex hull. Although compression enhances the ordering tendencies at Li-rich compositions, the Al_2Li_3 and Al_4Li_9 phases remain stable with respect to the bcc and fcc superstructures. Therefore, the DO_3 phase, even at high pressure, is still not a stable phase. As one might expect on the basis of a naive dense packing argument, the structural energy difference between fcc and bcc shifts in favor of the fcc structure at this high pressure both for pure Al and pure Li. At pressures over 2 GPa, Mehl[34] has found that bcc Li becomes mechanically unstable because the shear modulus, $C_{11} - C_{12}$, vanishes. In other recent work too[35], it has been shown that a given element or intermetallic compound may not be mechanically stable in certain crystal structures. Here we will only consider sta-

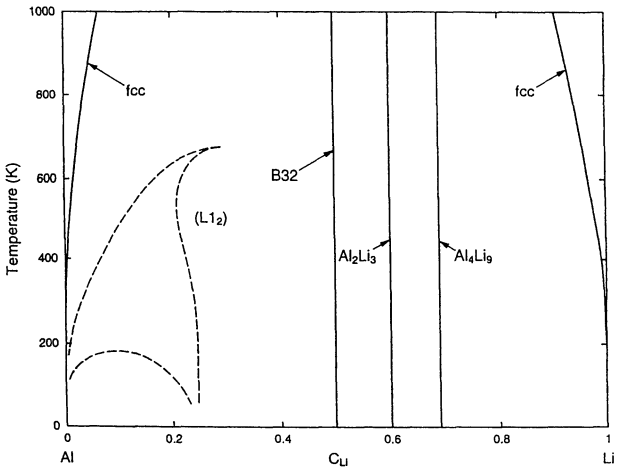

FIG. 4. The solid portion of the Al-Li phase diagram at 5.4 GPa hydrostatic pressure; binodals (solid lines), metastable phase boundaries (dashed lines).

bility with regards to isotropic deformations and short- and long range ordering. This means that when a phase is found to be stable, it still can be unstable with respect to a degree of freedom not considered here.

Considering the rather minor changes in the computed relative stability of the various ordered states it is not surprising that the predicted Al-Li phase diagram changes little with pressure. The most significant change at 5.4 GPa is a 35 % reduction of the Li solubility in fcc Al (see Figure 4). Indeed, experiments and a simple argument based on experimentally measured parameters[2] indicate that at a given temperature the Li solubility limit should decrease with pressure. At 600 °C the experimentally observed reduction is about 25 %[2].

It has been shown that under compression Al-Li alloys can be prepared with much higher Li concentrations in the fcc SS[2] than is possible under ambient pressures. This is due to the great increase in the melting temperature of Al-rich Al-Li alloys under pressure. The large melting point increase in turn is caused by the large expansion of Al-rich alloys upon melting.

The strong ordering tendencies of < 100 > type in Al-rich fcc alloys contradict some results reported with the KKR-ASA-CPA-GPM[36]. In that work strong phase separation tendencies are computed. This result must be incorrect because the ordered $L1_2$ phase is (meta)stable, and because several independent local density approximation calculations, including this work, have shown that the $L1_2$ phase is stable with respect to phase separation on the fcc lattice[9,37,34].

IV. CONCLUSION

The solid-phase portion of the Al-Li composition-temperature phase diagram has been computed from first principles at zero pressure and at 5.4 GPa. Although this calculation does not contain adjustable parameters, the result agrees well with available experimental observations. Specific correct features of the calculation are: 1) Close-packed structures for both pure Al and Li are more stable than bcc at zero temperature. 2) The lattice stability difference for Li at 0 K between bcc and fcc is small enough to be compensated for by vibrational contributions at higher temperatures in favor of the more "open" bcc structure. 3) The B32 structure is much more stable than other equi-atomic ordered configurations, such as B2, B11, $L1_0$ and K40. 4) The Al_3Li - $L1_2$ phase exists as a metastable ordered state. 5) The calculated congruent order-disorder temperature of the metastable Al_3Li - $L1_2$ phase falls within the wide scatter of its experimental determination. 6) The fcc - Al_3Li $L1_2$ two phase field has the correct width. 7) The misfit between the Al-rich SS and the Al_3Li - $L1_2$ phase is very small and negative. 8) Li is highly soluble in fcc Al and Al is rather insoluble in Li. 9) The AlLi phase (B32) is so stable that it melts before disordering takes place. 10) There is a low-temperature MG in Al-rich alloys, which is metastable with respect to the metastable order/disorder fcc phase separation. 11) The bulk modulus decreases with increasing Li content. 12) The Al_2Li_3 and Al_4Li_9 "interloper" phases are stable. Clearly, the phase diagram computed in this work is in much better qualitative and quantitative agreement with experiment than the previous *ab initio* result[9].

A remaining shortcoming is that the vibrational degrees of freedom are not considered. As a result, the fcc-bcc transformation in pure Li is not modeled, and the Li solubility in fcc Al-rich SS may be underestimated. Another quantitative shortcoming of the first-principles phase diagram is the underestimated width of the B32 single phase region. The computed width is less than 1 % at all temperatures below the actual melting point, whereas the assessment gives a maximum width of 8 %[5]. This discrepancy may be due to an overestimated formation energy of the Al_2Li_3 phase, or may result from inaccuracies in the assessment. The latter is possible because there is experimental data that suggests a much narrower single phase region (see figure 3 in Ref.[5]).

Our calculations indicate that the Al-Li system should not be strongly affected by hydrostatic compression. Only very minor effects, such as the reduced Li solubility in the Al-rich fcc SS are predicted. The computed reduction of the Li solubility at 5.4 GPa is about 35 %, in reasonable agreement with a recent measurement of 25 %[2]. We also predict that compression should very slightly enhance the solubility of Al in Li.

In the case of Cu-Be the results are not good. Although the computed enthalpies of formation for fcc-based phases are reasonable, those for bcc-based phases appear to be much too negative. This leads to an overestimation of the B2 order-disorder temperature and an underestimation of the Be solubility in the fcc Cu-rich matrix. However, the Cu-Be is a challenging system be-

cause the Calphad approach too, while achieving a good fit to the experimental phase diagram, gives rather unusual features in the compositional dependence of the entropy of mixing.

In spite of the failure to compute the Cu-Be phase diagram, the small predictive errors in both the Al-Li and Cu-Be systems indicate that an accurate cluster expansion for the configurational energy can be obtained using the total energies of about 10-20 ordered configurations only.

V. ACKNOWLEDGMENTS

The authors thank Dr. M. van Schilfgaarde for providing LMTO-ASA programs, and M.S. gratefully acknowledges the visiting professorship funded by Hitachi Corporation and the hospitality of the Institute for Materials Research at Tohoku University.

---

* Present Address: Brookhaven National Laboratory, Dept. of Physics, Upton, NY 11973-5000, USA.

[1] V.A. Phillips, Acta Met. **9** (1961), 216.
[2] A. Matsumuro, K. Sakai, M. Senoo, J. Mater. Sci. **28** (1993), 6567.
[3] M.L. Saboungi and C.C. Hsu, Calphad **1** (1977), 237.
[4] R.P Elliott and F.A. Shunk, Bull. Alloy Phase Diagrams **2** (1981), 353.
[5] A.J. McAlister, Bull. Alloy Phase Diagrams **3** (1982), 177.
[6] F.W Gayle and J.B. van der Sande, Bull. Alloy Phase Diagrams **5** (1984), 19.
[7] C. Sigli and J.M. Sanchez, Acta Metall. **34** (1986), 1021.
[8] A.G. Khachaturyan, T.F. Lindsey and J.W. Morris Jr., Met. Trans. **19A** (1988), 249.
[9] M. Sluiter, D. de Fontaine, X.Q. Guo, R. Podloucky, and A.J. Freeman, Phys. Rev. B **42** (1990), 10460.
[10] J.S. Garland and J.M. Sanchez, in *Kinetics of Ordering Transformations in Metals*, ed. H. Chen and V.K. Vasudevan, (TMS, Warrendale PA, 1992), 207.
[11] L. Kaufman and L.E. Tanner, Calphad **8** (1984), 121.
[12] D.J. Chakrabarti, D.E. Laughlin, and L.E. Tanner, Bull. Alloy Phase Diagrams **8** (1987), 269.
[13] H.L. Skriver, *The LMTO Method*, Springer series in Solid State Sciences, vol. **41**, (Springer, Heidelberg, 1983); O.K. Anderson, O. Jepsen, and D. Glotzel, in *Highlights of Condensed Matter Theory*, Internat. School of Phys. Enrico Fermi, Course **89**, eds. F. Bassani, F. Fermi, and M.P. Tosi, (North Holland, Amsterdam, 1985), 59.
[14] M. Asta, D. de Fontaine, M. van Schilfgaarde, M. Sluiter, and M. Methfessel, Phys. Rev. B **46** (1992), 5055.
[15] R. McCormack, M. Asta, D. de Fontaine, G. Garbulski, and G. Ceder, Phys. Rev. B **48** (1993), 6767.
[16] C. Wolverton, G. Ceder, D. de Fontaine, and H. Dreysse, Phys. Rev. B **45** (1992), 13105.
[17] C. Amador, W.R.L. Lambrecht, M. van Schilfgaarde, and B. Segall, Phys. Rev. B **47** (1993), 15276.
[18] Z.W. Lu, S.-H. Wei, and A. Zunger, Europhys. Lett. **21** (1993), 221.
[19] P.P. Singh, A. Gonis, P.E.A. Turchi, Phys. Rev. Lett. **71** (1993), 1605.
[20] D.D. Johnson, J.B. Staunton, and F.J. Pinski, Phys. Rev. B **50** (1994), 1473.
[21] Z.W. Lu, S.H. Wei, and A. Zunger, Phys. Rev. B 44 (1991), 512.
[22] R. Kikuchi, Phys. Rev. **81** (1951), 988.
[23] D. de Fontaine, in *Solid State Physics*, vol. **34**, ed. by H. Ehrenreich, F. Seitz, and D. Turnbull (Academic Press, New York, 1979), 1.
[24] J.M. Sanchez, F. Ducastelle and D. Gratias, Physica A**128** (1984), 334.
[25] H.G. Smith, Phys. Rev. Lett. **58** (1987), 1228.
[26] J.W. Connolly and A.R. Williams, Phys. Rev. B **27** (1983), 5169. D. de Fontaine, in *Solid State Physics*, vol. **47**, ed. by H. Ehrenreich and D. Turnbull (Academic Press, New York, 1994), 80.
[27] M. Sluiter, Y. Watanabe, D. de Fontaine, and Y. Kawazoe, Phys. Rev. B, accepted (1996).
[28] T. Mohri, J.M. Sanchez, and D. de Fontaine, Acta Metall. **33** (1985), 1171.
[29] J. Kanamori and Y. Kakehashi, J. Phys. (Paris), Colloq. **38** (1977), C-7-274.
[30] A. Finel and F. Ducastelle, in *Phase Transformations in Solids*, T. Tsakalakos ed. (North-Holland, Amsterdam, 1984), 293.
[31] H.J. Saunders, A.P. Miodownik, and A.T. Dinsdale, Calphad **12** (1988), 351.
[32] R. Hultgren, P.D. Desai, D.T. Hawkins, M. Gleiser, and K.K. Kelley, *Selected Values of the Thermodynamic Properties of Metals and Binary Alloys*, (ASM, Metals Park, OH, 1973), 370.
[33] G.D. Garbulski and G. Ceder, Phys. Rev. B **49** (1994), 6327.
[34] M. Mehl, Phys. Rev. B **47** (1993), 2493.
[35] P.J. Craievich, M. Weinert, J.M. Sanchez, and R.E. Watson, Phys. Rev. Lett. **72** (1994), 3076.
[36] A. Gonis, P.E.A. Turchi, M. Sluiter, F.J. Pinski, D.D. Johnson, Mat. Res. Soc. Symp. Proc. vol. **186**, eds. G.M. Stocks, D.P. Pope, A.F. Giamei, (1990), 89, fig. 3 and 4.
[37] K.I. Masuda-Jindo and K. Terakura, Phys. Rev. B **39** (1989), 7509.
[38] L. Kaufman and H. Bernstein, *Computer Calculation of Phase Diagrams*, (Academic Press, NY, 1970).
[39] P.E.A. Turchi, M. Sluiter, F.J. Pinski, D.D. Johnson, D.M. Nicholson, G.M. Stocks, and J.B. Staunton, Phys. Rev. Lett. **67** (1991) 1779, and erratum ibid **68** (1992), 418.